Printing Chemical Gradients

Tobias Kraus,[†,‡] Richard Stutz,[†] Tobias E. Balmer,[‡] Heinz Schmid,[†] Laurent Malaquin,[†] Nicholas D. Spencer,[‡] and Heiko Wolf*[,†]

IBM Research GmbH, Zurich Research Laboratory, Säumerstrasse 4, CH-8803 Rüschlikon, Switzerland, and Laboratory for Surface Science and Technology, Department of Materials, Swiss Federal Institute of Technology ETH, Hönggerberg, Wolfgang-Pauli-Strasse 10, CH-8093 Zürich, Switzerland

Received March 10, 2005. In Final Form: June 1, 2005

We describe a method to exploit the mass-transfer limitations of microcontact printing for the fabrication of surfaces with well-defined, arbitrarily shaped composition variations. An analysis of the transport processes reveals that the printing of hexadecanethiol (HDT) from poly(dimethylsiloxane) is purely diffusion-controlled. Stamps with geometries that enhance surface-normal diffusion paths therefore allow not only the contours, but also the local density of self-assembled monolayers to be controlled. We use stamps with variable thickness and uniform ink concentration to print HDT density gradients on gold, depleting the stamps during the process. In the second step, a perfluorinated thiol fills the vacancies in the partial monolayer to form a two-component gradient that we analyze by means of X-ray photoelectron spectroscopy and spectroscopic ellipsometry. Linear and radial gradients are shown here as examples for a wide range of geometries that can be fabricated with high precision using the method.

1. Introduction

Microcontact printing (μCP) has been applied with considerable success to the chemical patterning of surfaces. Etch susceptibility, biological functionality, surface energy, and other surface properties can be efficiently modulated at a high resolution down to tens of nanometers.[1,2] The method can define structures with high contrast and sharp contours.

Here we present a related technique that complements the "binary" surface patterning of μCP in the same way that grayscale lithography complements standard photolithography. We exploit the unique capability of the silicone elastomer poly(dimethylsiloxane) (PDMS) to dissolve certain alkanethiols and leave them mobile in the bulk material. If the amount of thiol in the stamp is smaller than that in a full monolayer and the deposited amount depends on the position, we can print "analog" patterns on surfaces, i.e., surface−composition gradients with defined spatial evolution. Such gradients are of interest for the biological sciences, both in studies of cell adhesion and movement. They also allow surface adsorption experiments (widely used in many fields) to be performed over a wide range of conditions on a single sample. Finally, the gradients can be used to control fluid movement, with potential applications ranging from microfluidics to self-assembly.

Various examples for the preparation of gradients have been published. A review by Ruardy et al.[3] includes methods based on diffusion in ambient air or a gel on the substrate, moving liquid menisci, as well as moving plasma sources. A particularly simple method is the slow immersion of the sample into a solution that was demonstrated by Morgenthaler et al.[4] Electrochemical methods based on the partial desorption of molecules depending on their position[5] have been used as well as microfluidic systems.[6,7] Choi and Newby recently showed how to use printing-time variations in μCP to create steep, stepped gradients on silicon.[8] Grzybowski's group has used printing with controlled diffusion and reaction to prepare color patterns[9] as well as surface topographies.[10] They used gels that can dissolve inorganic ions which upon printing react with other ions dissolved in the substrate.

In our case, reaction only occurs at the surface of the substrate, similar to the situation in standard μCP. The stamps are thinner than those used usually, and their thickness varies over the surface. Printing is done as in conventional μCP, but the diffusion and reaction behavior of the printed thiol allow us to control the amount of thiol at each point of the surface. The resulting pattern corresponds to the stamp geometry.

In the first part of this paper, an analysis of the mass-transfer characteristics demonstrates that the process is mainly diffusion-controlled. From this knowledge we derive rules for the design of stamps having geometries that govern the amount of locally transferred thiol. We describe the use of such stamps in the second part for printing linear gradients that we characterize in detail using X-ray photoelectron spectroscopy (XPS). The results indicate that arbitrary shapes are possible, including radial gradients that are shown as an example.

* Corresponding author. E-mail: hwo@zurich.ibm.com.
† IBM Research GmbH, Zurich Research Laboratory.
‡ Swiss Federal Institute of Technology.

(1) Xia, Y. N.; Whitesides, G. M. *Angew. Chem., Int. Ed.* **1998**, *37*, 551−575.
(2) Michel, B.; Bernard, A.; Bietsch, A.; Delamarche, E.; Geissler, M.; Juncker, D.; Kind, H.; Renault, J.; Rothuizen, H.; Schmid, H.; Schmidt-Winkel, P.; Stutz, R.; Wolf, H. *IBM J. Res. Devel.* **2001**, *45*, 697−719.
(3) Ruardy, T.; Schakenraad, J. M.; vanderMei, H.; Busscher, H. *Surf. Sci. Rep.* **1997**, *29*, 3−30.
(4) Morgenthaler, S.; Lee, S. W.; Zürcher, S.; Spencer, N. D. *Langmuir* **2003**, *19*, 10459−10462.
(5) Terrill, R. H.; Balss, K. M.; Zhang, Y. M.; Bohn, P. W. *J. Am. Chem. Soc.* **2000**, *122*, 988−989.
(6) Jeon, N. L.; Dertinger, S. K. W.; Chiu, D. T.; Choi, I. S.; Stroock, A. D.; Whitesides, G. M. *Langmuir* **2000**, *16*, 8311−8316.
(7) Fosser, K. A.; Nuzzo, R. G. *Anal. Chem.* **2003**, *75*, 5775−5782.
(8) Choi, S. H.; Newby, B. M. Z. *Langmuir* **2003**, *19*, 7427−7435.
(9) Klajn, R.; Fialkowski, M.; Bensemann, I. T.; Bitner, A.; Campbell, C. J.; Bishop, K.; Smoukov, S.; Grzybowski, B. A. *Nat. Mater.* **2004**, *3*, 729−735.
(10) Campbell, C. J.; Baker, E.; Fialkowski, M.; Grzybowski, B. A. *Appl. Phys. Lett.* **2004**, *85*, 1871−1873.

10.1021/la0506527 CCC: $30.25
Published on Web 07/13/2005

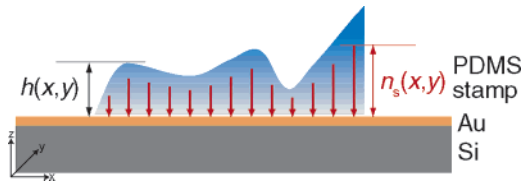

Figure 1. Principle of diffusion-controlled depletion printing. The stamp thickness $h(x, y)$ directly governs the amount of substance $n_s(x, y)$ transferred to each part of the surface.

2. Mass-Transfer Analysis

To a first approximation, the amount of a thiol n_s that is transferred from a stamp to a gold surface, where it forms a (partial or full) self-assembled monolayer, is controlled by the initial concentration c_0 inside the stamp and the thickness of the stamp

$$n_s(x, y) = \int_0^{h(x,y)} c_0(x, y, z)\, dz \tag{1}$$

Both of these quantities can, in principle, be varied in order to control the final surface composition. However, it is difficult to ink a stamp with a defined concentration pattern. The basic idea of our method is therefore to prepare a stamp with variable thickness h over its area of contact, $h = h(x, y)$. Ideally, the printed amount at a specific point of the surface produced then only depends on the height of the stamp above this point Figure 1:

$$n_s(x, y) = h(x, y)c_0 \tag{2}$$

The above equation is applicable if during the printing process most of the molecules travel toward the surface vertically. This is only possible if diffusion (and not reaction) limits the monolayer formation. Several groups have found the process of monolayer formation from ethanol solution to be diffusion-limited.[11,12] As the diffusion constant of hexadecanethiol (HDT) in PDMS is 1 order of magnitude lower than in ethanol,[13] one might expect that the formation of monolayers from PDMS stamps is diffusion-limited as well. However, further inspection shows that the situation is somewhat more complex in our case: even if the initial rate of monolayer formation is high, it will drop considerably while achieving full coverage. At the same time, the concentration inside the stamp decreases. We will provide a more quantitative treatment in the following that takes the thickness of the stamp into account.

2.1. Diffusion Limit of Monolayer Formation. The transport of thiol inside the stamp is described by Fick's second law of diffusion[13]

$$\frac{\partial c}{\partial t} = D\nabla^2 c \tag{3}$$

which deals with the temporal evolution of the solute concentration c in a material where the solute has a constant diffusion coefficient D.

We use dimensionless variables in the following. A characteristic diffusion time t^* for a stamp of thickness h is $t^* = h^2/D$, so that we express time as $\tau \equiv tD/h^2$. The surface-normal coordinate becomes $\zeta \equiv z/h$ and the lateral coordinate $\xi \equiv x/h$. Concentrations are normalized to the initial concentration, $\Theta \equiv c/c_0$. For the two-dimensional case, eq 3 becomes

$$\frac{\partial \Theta}{\partial \tau} = \frac{\partial^2 \Theta}{\partial \xi^2} + \frac{\partial^2 \Theta}{\partial \zeta^2} \tag{4}$$

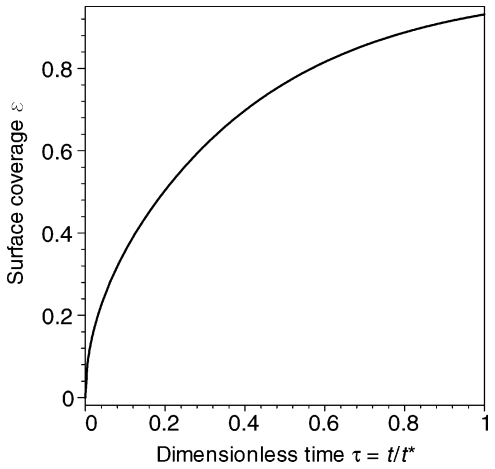

Figure 2. Change of surface coverage in an entirely diffusion-controlled printing process.

Let us assume that the rate of monolayer formation is governed by diffusion and that the reaction is rapid enough to model the gold surface as a perfect thiol sink. A stamp of constant thickness is then adequately represented by the one-dimensional version of eq 4 with a zero-concentration boundary condition on its printing side and a zero-flux boundary condition on its other side.

An analytical solution for diffusion in a slab between $\zeta = -1$ and 1 with constant-concentration boundary conditions of $\Theta_{\zeta=\pm1} = 0$ and a uniform initial concentration c_0 is given by Crank[14] as an infinite series

$$\Theta = \frac{4}{\pi}\sum_{n=0}^{\infty} \frac{(-1)^n}{2n+1} \exp\left(-\frac{(2n+1)^2\pi^2\tau}{4}\right) \cos\left(\frac{(2n+1)\pi}{2}\zeta\right) \tag{5}$$

Owing to symmetry, there is no flux across $\zeta = 0$. One-half of the solution where $1 > \zeta > 0$ can thus be used as model for the thick part of the actual stamp. The dimensionless diffusive flux $\psi_{\text{diffusion}}$ through the surface toward the substrate is then

$$\psi_{\text{diffusion}} = -\frac{\partial \Theta}{\partial \zeta}\Big|_{\zeta=1} = -2\sum_{n=0}^{\infty} \exp\left(-\frac{(2n+1)^2\pi^2\tau}{4}\right) \tag{6}$$

According to our assumption, the full diffusive flux is adsorbed onto the substrate. Numerical evaluation shows that the fraction of surface covered ϵ then changes according to Figure 2.

2.2. Reaction Limit of Monolayer Formation. The above result indicates the maximum amount of thiol that can be transported toward the interface. Another possible limit for the overall speed is the adsorption reaction with its finite reaction rate that depends on the surface thiol concentration.

We follow Jung and Campbell[15] and state the surface reaction rate R_{ads} in terms of a sticking probability S that

(11) Camillone, N. *Langmuir* **2004**, *20*, 1199−1206.
(12) Jung, L. S.; Campbell, C. T. *Phys. Rev. Lett.* **2000**, *84*, 5164−5167.
(13) Balmer, T. E.; Schmid, H.; Stutz, R.; Delamarche, E.; Michel, B.; Spencer, N. D.; Wolf, H. *Langmuir* **2005**, *21*, 622−632.
(14) Crank, J. *The Mathematics of Diffusion*; Oxford University Press: New York, 1964.
(15) Jung, L. S.; Campbell, C. T. *J. Phys. Chem. B* **2000**, *104*, 11168−11178.
(16) Larsen, N. B.; Biebuyck, H.; Delamarche, E.; Michel, B. *J. Am. Chem. Soc.* **1997**, *119*, 3017−3026.

decreases from S_0 whereas the fraction of surface covered, ϵ, increases from zero (to a maximum of unity for a full monolayer)

$$R_{ads} = S_0(1 - \epsilon)c_{thiol}\sqrt{\frac{k_B T}{2\pi m}} \quad (7)$$

where c_{thiol} is the concentration of free thiol at the surface, k_B the Boltzmann constant and m the mass of a molecule. [These adsorption kinetics have been established for the formation of monolayers from ethanol. The conformal contact between PDMS and gold and the high mobility of HDT in the silicone lead to a comparable adsorption situation. Printed monolayers are identical in structure to those obtained from solution.[16]] The reactive flux to the surface $J_{reaction}$ reaches the surface at most until a full monolayer with a surface concentration c_{ML} has been reached so that we can state

$$\epsilon(x, t) = \frac{\int_0^t J_{reaction}(x, t')\,dt'}{c_{ML}} \quad (8)$$

For an entirely reaction-limited system where the thiol can diffuse in the stamp infinitely rapidly, the surface concentration Θ_s of free thiol decreases at the same rate as the surface coverage ϵ of the monolayer increases: $\Theta_s = 1 - \epsilon$. The reaction-limited flux toward the surface in dimensionless form $\psi_{reaction}$ is then

$$\psi_{reaction} = S_0(1 - \epsilon)^2\frac{h}{D}\sqrt{\frac{k_B T}{2\pi m}} \quad (9)$$

Thermodynamic data suggest that very little thiol will be left in the stamp when the chemical equilibrium is finally reached. From literature values[17] of the desorption enthalpy we can calculate the equilibrium constant to be on the order of $K \approx 3 \times 10^{22}$. [Details of the calculation can be found in the Supporting Information.] The concentration of free thiol at an initial concentration of 1 μmol/L then becomes negligible ($c \leq 10^{-23}$ mmol/L).

2.3. Comparison of Diffusive and Reactive Limits. The surface reaction might not be fast enough to immediately consume that part of the substance that diffuses to the surface. By comparing the kinetics of monolayer formation to the diffusive flux, we identify the actual rate-limiting step that controls the monolayer formation in the printing process.

Figure 3 shows the maximum reactive flux as well as the maximum flux that can be reached with an actual PDMS stamp, as obtained from eq 6. The reaction can take up considerably more thiol than diffusion can provide during most of the process. Only in the very beginning (where the "fresh stamp" comes in contact with the gold) and toward the very end (where the concentrations become very low and the reaction slows down) might the reaction briefly limit monolayer formation. For the largest part, printing is diffusion-limited. Although we have shown this for the thickest part of the stamp, the conclusion also holds for the thin parts.

2.4. Applicability of the Perfect Sink Model. There remains the question of how close the actual situation is to the diffusion limit. The concentration of free thiol at the stamp−gold interface does not drop to zero as we had assumed for the calculation of the upper mass transfer limit. It is also smaller than it would be for a stamp with

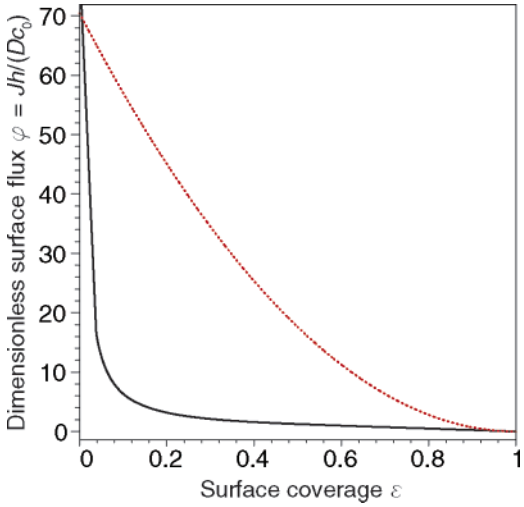

Figure 3. Flux of thiol toward the gold surface for a hypothetical reaction-limited (dashed line) and the diffusion-limited (solid line) process.

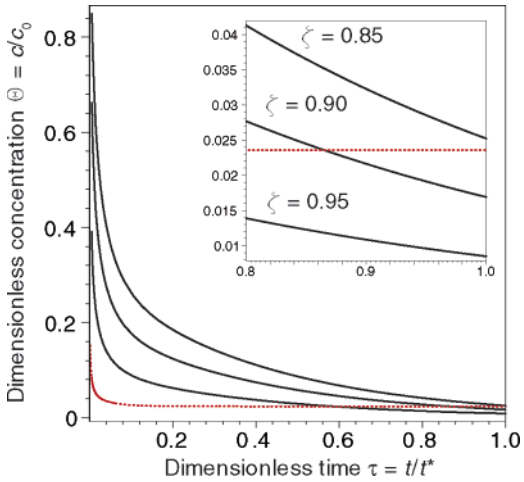

Figure 4. Comparison of solute concentrations inside the stamp for an infinitely rapid surface reaction at different locations close to the surface (solid line) to the "kinetic" concentration required to take up all substance (dashed line).

an infinite diffusion coefficient of thiol. We can estimate the deviation from the assumed concentration profile by numerical evaluation of the concentration terms in both the diffusion and the kinetic equations. The comparison of these concentrations then leads to the plot in Figure 4. During most of the printing time, i.e., until a coverage of about 80% is reached according to Figure 2, the concentration very close to the surface of our above-mentioned model is higher than required for the reaction to take up all of the thiol diffusing toward the surface. This is equivalent to saying that the depletion layer that is commonly used in liquid systems as a measure for the diffusion limitation of the total process[18] is as thick as the entire stamp during most of the printing process. The actual situation is therefore close to the diffusion model described above.

Toward the end of printing, the kinetics of monolayer formation change: Equation 7 is probably not valid for surface coverage above 80% where a slower formation process has been reported.[17] At the same time, concentra-

(17) Bain, C. D.; Troughton, E. B.; Tao, Y. T.; Evall, J.; Whitesides, G. M.; Nuzzo, R. G. *J. Am. Chem. Soc.* **1989**, *111*, 321−335.

(18) Bond, W. N.; Puls, H. O. *London*, *Edinburgh*, *Dublin Philos. Mag. J. Sci.* **1937**, *24*, 864−888.

(19) Liao, Y. C.; Franses, E. I.; Basaran, O. A. *J. Colloid Interface Sci.* **2003**, *258*, 310−321.

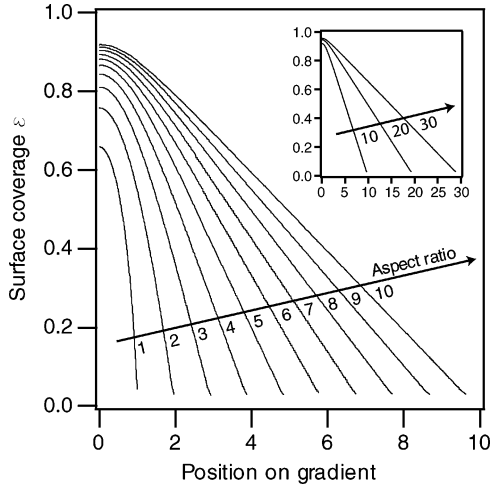

Figure 5. Calculated amounts of thiol adsorbed from the stamp at different positions along the gradient, for stamps with aspect ratios from 1 to 10 (higher ratios are shown in the inset). A full monolayer is reached at a dimensionless concentration of unity.

tions inside the stamp reach levels that are so low that diffusion control is not necessarily maintained. Comparing the amounts transferred, we can expect that the influence of this last phase is much smaller than that of lateral diffusion during the main part of printing. We will therefore model the entire printing process purely based on diffusion with a zero-concentration boundary condition at the interface.

2.5. Stamp Design. Several constraints have to be taken into account in the design of the stamp. We will provide some design rules in the following.

Maximum Gradient Steepness. During the depletion of the stamp, diffusion will not only transfer ink toward the surface but also distribute it laterally, effectively smoothing the gradients to be printed. This limits the steepness of the surface composition gradient that can be printed. The effect is most easily seen for a linear gradient obtained from a wedge-shaped stamp: The aspect ratio of such a stamp (length to thickness) has to be larger than unity to obtain a linear gradient.

To be more quantitative, we analyze the interplay of lateral and normal diffusion. A two-dimensional finite element method (FEM) discretization of eq 4 for a stamp with triangular cross section reveals the limitations of our method. As the process proceeds at the upper diffusion limit according to the above results, a simple sink condition at the gold surface is sufficient for modeling. [The combination of diffusion and reaction processes using FEM has been demonstrated[19] but introduces a high level of complexity to the model.]

All calculations to find a finite element solution of diffusive transport inside the wedge were performed using MatLab (The MathWorks, Natick, MA). The diffusive flux through the contact area arises from the concentration gradient in the elements close to the edge. We calculated it for every time step and balanced it with the content of the stamp to check for consistency. Integration over all time steps for every element at the boundary at the edge then yielded the amount of substance absorbed at this point.

Figure 5 shows the printed amount in dependence of the normalized coordinate along the gradient for wedge-shaped stamps with different aspect ratios. All of them contained enough ink to establish a full monolayer at their thick end (corresponding to a dimensionless surface concentration of unity). Small aspect ratios lead to considerable lateral diffusion inside the stamp and thus nonlinear gradients. At an aspect ratio of 10, the gradients become fairly linear. Only in the thick part of the stamp remains a slight "bulging", even in long gradients (aspect ratio of 100). The thin ends of the high-aspect-ratio stamps exhibit artifacts of the FEM mesh and have been removed in the plot.

Thiol Concentration. The amount of thiol required to form a monolayer has to be soluble in the stamp. If one molecule in the self-assembled monolayer covers an area of 0.21 nm^2 (as reported by Dubois and Nuzzo[20]), we require an amount of 7.9 $\mu mol/m^2$. The solubility of HDT in polydimehylsiloxane (PDMS) was given by Balmer et al.[13] as 486 mol/m^3, so that the minimum thickness is on the order of tens of nanometers. All stamps used in practice are considerably thicker.

Printing Time. The maximum thickness of the stamp has to be small enough to allow all of the substance to diffuse onto the surface in a reasonable time. In addition, it has to be possible to prepare an ink pad of reasonable thickness with the same concentration in the manner described in the Experimental Section.

The characteristic diffusion time $t^* = h^2/D$ provides a rough estimate of the printing time required. In the case of HDT in PDMS with a diffusion coefficient of[13] $D = 5.9 \times 10^{-11}$ m^2/s, a reasonable stamp thickness is 50 μm, corresponding to a characteristic time of 42 s. Note that this time is independent of the initial concentration. It indicates when a considerable part of the thiol (roughly 90%) has left the stamp.

3. Experimental Results

We printed various gradients using appropriate stamps to verify our theoretical calculations and optimize the process. The stamps were fabricated by casting PDMS in microfabricated molds. Wedge-shaped stamps for the printing of linear gradients were removed from their mold and used on glass carriers, conical stamps were left in their metal mold.

Prior to printing, we placed the stamps on large PDMS slabs (ink pads) with defined thiol concentrations so that they equilibrated to a known thiol content (Figure 6, step 1). Such slabs have a thiol content that is large compared with that of the stamps. They can be inked with high precision to a uniform thiol concentration throughout the entire slab in reasonable time.[21] Both precise concentration and uniformity are prerequisites for the gradient printing, even more so than in conventional μCP.

On contact with a gold surface, the stamp formed HDT gradients (Figure 6, step 2). Immediately afterward, we backfilled the vacant gold surface with perfluorododecanethiol (PFDDT) (Figure 6, step 3). This creates a surface composition gradient at low surface energy levels that is stable for several days at least. The fluorine content of the complementary monolayer is readily detected using XPS for the characterization.

3.1. Gradient Characterization. X-ray photoelectron spectroscopy, spectroscopic ellipsometry (SE), and contact angle measurements can be used to characterize the printed gradients. The fluorine contained in the PFDDT part of the monolayer causes a strong signal in XPS that is easily detected. [The F 1s signal is four times stronger than that of C 1s.] PFDDT monolayers also exhibit a distinct difference in refractive index and reduced thick-

(20) Dubois, L. H.; Nuzzo, R. G. *Ann. Rev. Phys. Chem.* **1992**, *43*, 437−463.

(21) Libioulle, L.; Bietsch, A.; Schmid, H.; Michel, B.; Delamarche, E. *Langmuir* **1999**, *15*, 300−304.

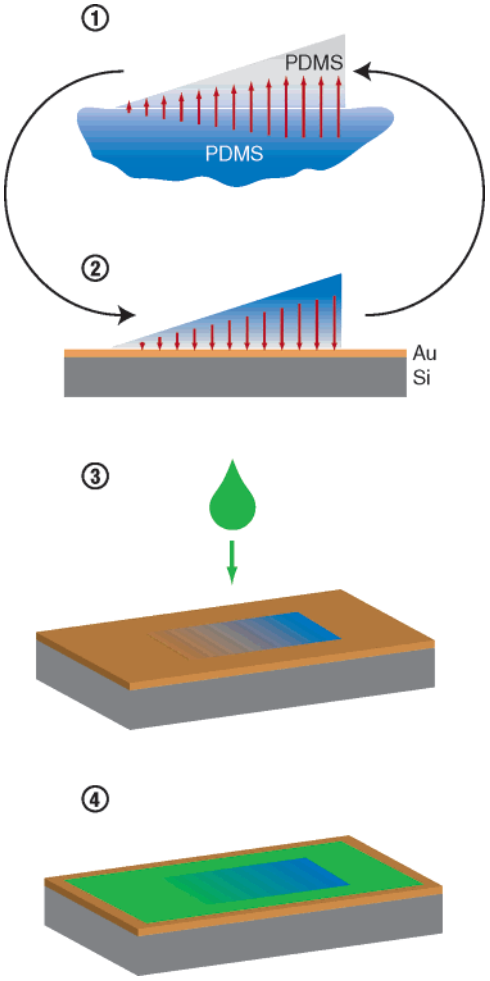

Figure 6. (1) Thiol diffuses into the stamp from an ink pad. (2) It leaves the stamp because of adsorption to the gold surface and creates a partially covered surface. (3) The voids can be filled with other thiols to form a two-component surface-composition gradient (4).

ness, both of which can be detected via ellipsometry. Finally, the surface energy difference between the fluorinated and the alkyl-terminated thiols can in principle be determined from the contact angle of sessile drops, although the spatial resolution is limited and the relation between surface energy and monolayer composition is not obvious. In practice, XPS provided the most efficient analytical method.

For the gradient analysis, we obtained survey spectra at a pass energy of 80 eV and high-resolution spectra of the Au4f, the C1s and the F1s regions at a pass energy of 40 eV for both reference and gradient samples. Beam-induced damage was expected to be small for our monochromatized source and was not observed during the measurements. To analyze the entire length of the gradient, we repeated the analysis at 14 or 15 points spaced 1 mm apart along its length.

The fraction of PFDDT in the monolayers can be obtained from XPS spectra either as the ratio of the measured F1s sample peak area to that of a full PFDDT monolayer or from the splitting of the C1s peaks that is caused by the strong chemical shift of C1s electrons in the neighborhood of C−F bonds (Figure 7). The former has the advantage of yielding a strong signal, the latter provides an internal C1s standard. However, the compound area of all C1s peaks changes from pure HDT to pure PFDDT layers so that this standard can be only used indirectly.

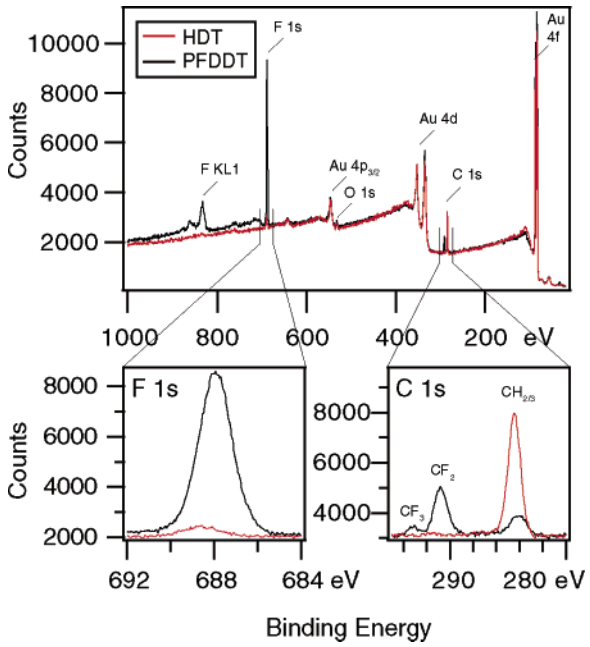

Figure 7. XPS signals acquired at the PFDDT end (black) and the HDT end (red) of a gradient.

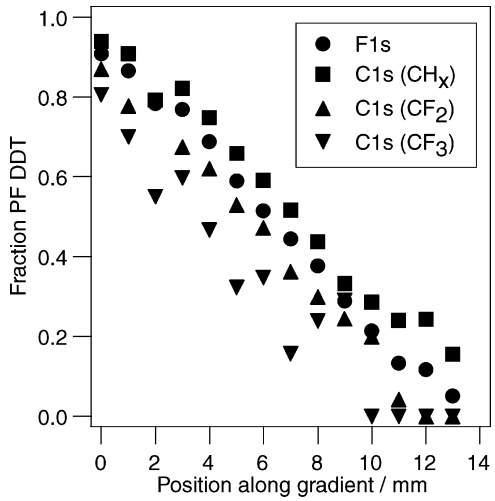

Figure 8. Comparison of surface composition according to different XPS peaks.

Figure 8 shows the composition of a HDT/PFDDT gradient at different positions as obtained from the analysis of different parts of the XPS signal. Different peaks are compared directly with the peaks measured on reference samples of pure HDT (no fluorine content) and PFDDT (maximum fluorine content). The change of the unshifted C1s signal systematically overestimates the PFDDT fraction, whereas the shifted C1s peaks (sometimes grossly) underestimates it. The fluorine peak seems to provide the best indication of PFDDT content, and the standard error of the mean over several independent measurements was found to be low. [More detailed error analysis of the different composition values can be found in the Supporting Information.]

Some gradients were also analyzed using SE. Figure 9 shows a (nonlinear) gradient composition derived from both XPS and ellipsometry data. The main difficulty in dealing with such data is that the thickness and the refractive index cannot be obtained simultaneously for such ultrathin films. This is particularly problematic because both parameters change with position in the

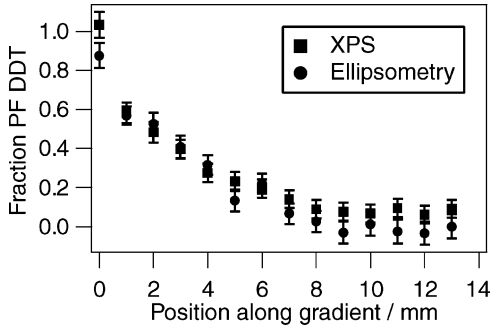

Figure 9. Surface composition gradient printed using a stamp with an overly high HDT concentration.The composition was analyzed using both XPS and ellipsometry. Error bars indicate the 90% confidence interval of the entire measurement for XPS data and the 90% confidence interval for the ellipsometry model fit.

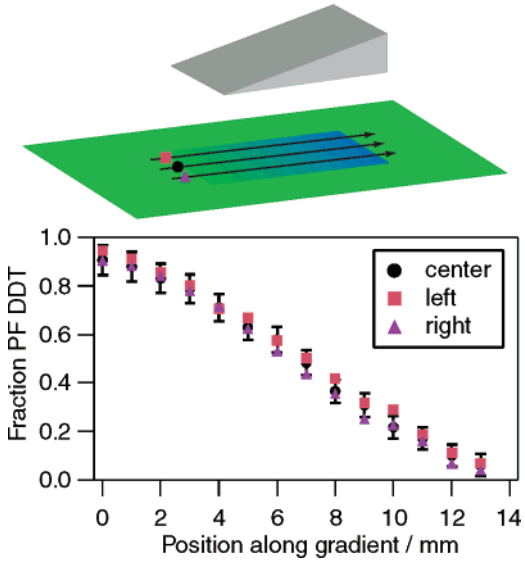

Figure 10. Surface composition according to XPS at three lateral positions along a single gradient.

gradient. We followed Bain and Whitesides,[22] and chose a thickness of the mixed monolayer of 1.88 nm that lies between the measured values for HDT and PFDDT monolayers. The exact value was chosen so that the fits converged. We then created a two-component model from reference data of pure HDT and PFDDT monolayers and used the fraction of PFDDT as the free variable for a fit. The results agree well with the composition derived from XPS, but the uncertainties connected with the fit are rather large. We therefore used XPS as our principal analytical tool.

3.2. Linear Gradients. Highly linear gradients were fabricated reproducibly using perfectly wedge-shaped stamps. The resulting surfaces show good uniformity in the lateral direction. Figure 10 shows results of XPS analysis along the center line of the stamped gradient (which was 5 mm in width) and at positions two millimeters to the left and right of the center line.

As predicted in the mass-transfer analysis, the stamp shape governs the resulting gradient evolution. This also accounts for some of the typical deviations from the desired shapes: shallow gradients from stamps with inadequate steepness and nonlinear gradients from stamps with bulges (Figure 11). The latter occurs when too high a stress

(22) Bain, C. D.; Whitesides, G. M. *J. Am. Chem. Soc.* **1989**, *111*, 7164−7175.

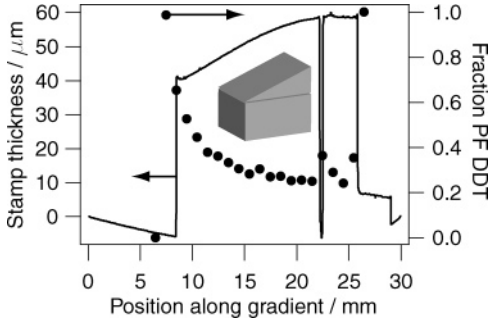

Figure 11. Profile of a defective stamp with little height variation. The surface composition gradient obtained is shallow.

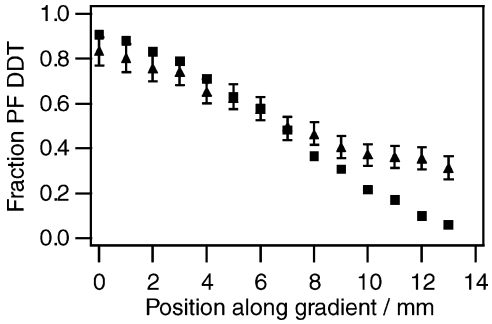

Figure 12. Surface composition according to XPS in two different linear gradients printed successively using the same stamp, with reinking. The thiol concentration in the second print (triangles) was slightly too low.

builds up in the polymer layer during fabrication. The printed gradient is a faithful representation of the deformed shape as long as the deformation allows the PDMS to establish conformal contact with the gold surface. Inspection of the stamps via profilometry identified such stamps so that we could avoid undesired geometrical effects.

In addition to stamp geometry, the overall concentration of the thiol in the stamp had a profound effect. A stamp would produce a gradient that is not as steep as expected if the thiol concentration was lower than optimal. Profiles of two different gradients made using the same stamp are shown in Figure 12. In the second print, only part of the surface composition range is present in the gradient. This deviation also occurs when the thiol concentration inside the stamp decreases owing to oxidation or evaporation of the ink.

In contrast, excessive concentrations led to steeper gradients with a saturated region of constant HDT coverage as shown in Figure 9 (although there still is some PFDDT present, *vide infra*). Here, the PDMS stamps still contain some thiol after printing. Multiple prints using a stamp with a very large initial HDT concentration of 200 μg/ml lead to a front that moved from print to print (Figure 13). The thin parts of the stamp were depleted soon, whereas the thick parts established a full monolayer and did not lose any solute thereafter. In this experiment, we kept the time between the prints as short as possible (approximately 1 min) to limit lateral diffusion.

All concentration effects are consistent with a very simple model that only takes into account surface-normal diffusion of the thiol. Figure 14 shows the three possible situations: (1) Insufficient concentration where the full gradient length is preserved, but the maximum coverage is not full and the dynamic range is limited; (2) adjusted concentration where the full gradient range is present; and (3) excessive concentration where part of the thick

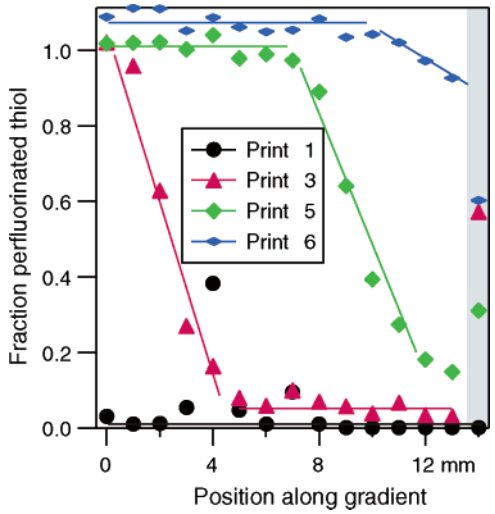

Figure 13. Surface composition gradients from different prints using the same stamp without reinking, starting at an excessive concentration of 200 μg/mL. Compositional values in the last millimeter (gray background) are subject to alignment errors between the XPS analysis spot and the gradient end. The lines serve as a guide to the eyes.

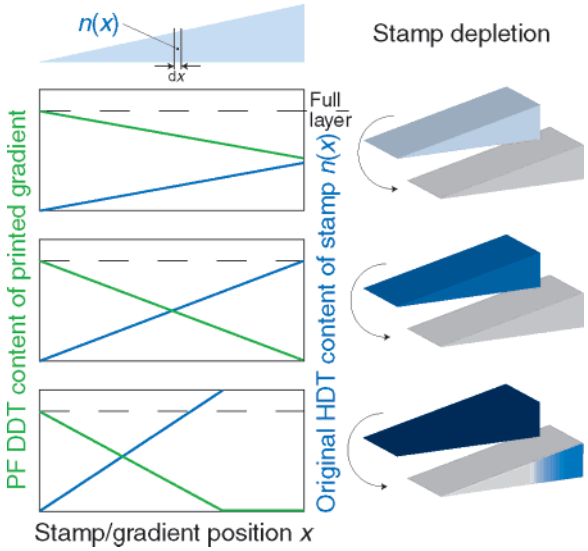

Figure 14. Relation between concentration and gradient shape. Low concentrations (top) lead to shallow gradients, adjusted concentrations (middle) allow full-length gradients with maximum dynamics, excessive concentrations (bottom) lead to steep gradients with saturation.

stamp end contains more material than can be adsorbed on the surface.

In most cases it will be desirable to use just enough thiol so that a full monolayer is reached at the very end of the gradient. We found a concentration of 40 μg/mL to provide satisfactory gradients from our 50 μm stamps. This leads to a surface concentration of 7 μmol/m^2 on the thick side of the stamp, slightly below the literature value[20] of 7.9 μmol/m^2 for a complete HDT monolayer.

XPS signals clearly reveal the presence of fluorinated thiol even in regions where full coverage by HDT is expected. This is likely not due to improper stamp concentration levels. Two other effects might be responsible for this deviation. The last 20% of the monolayer formation have been reported to be considerably slower than expected from first-order Langmuir kinetics.[17] Even though our printing time of 3 min is considerably longer than required for diffusion, it might not be sufficient to

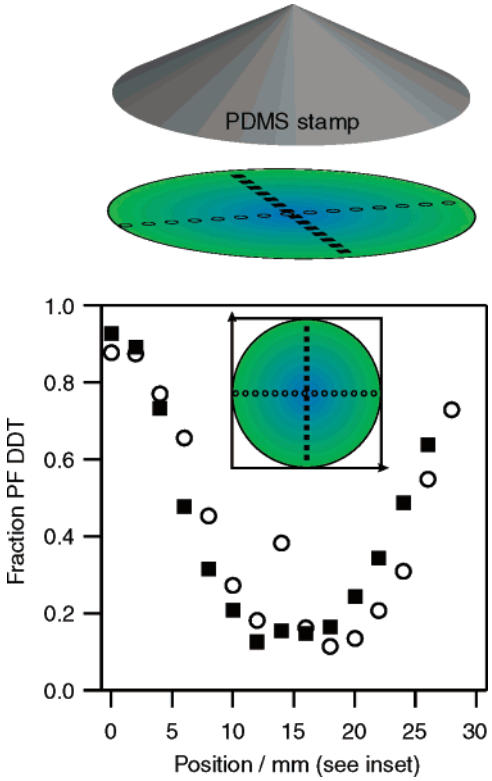

Figure 15. Surface composition gradient printed using a radial stamp. Measurement positions are indicated in the inset. The coordinate origin is at the lower left-hand corner.

form a perfect monolayer. However, the comparison of XPS data of reference monolayers to that of printed gradients does not indicate enough voids to account for the entire effect. [Reference samples were prepared from solution with long immersion time.] More important seems to be the replacement of adsorbed HDT molecules from the surface by PFDDT.[23] We found that reference monolayers of HDT that were treated with PFDDT in the same way exhibited 6% of PFDDT in the monolayer. We thus optimized the second adsorption step so that it filled as large a fraction of the uncovered surface while replacing as little of the existing monolayer as possible. Best results were achieved using a short treatment (about 20 s) with a solution of PFDDT (0.4 g/L) in dichloromethane. A heavily fluorinated solvent could cause contamination of the surfaces by fluorine-containing residues and disturb the analysis.

3.3. Radial Gradients. Other stamp geometries enable both nonlinear gradient contours and profiles. We prepared radial gradients that symmetrically fell off from the center. The mold for the stamp used had a conical recess with a central protruding pin from machining. The maximum depth was 100 μm so that we had to halve the ink concentration and increase the equilibration times by a factor of 4. The XPS analysis results in Figure 15 reveal that there was a "plateau" in the center of the printed area, interrupted by a hole (most likely due to the above-mentioned pin in the mold). The low-fluorine plateau is probably due to a slight excess in HDT concentration inside the stamp, analogously to what has been observed for linear gradients.

Liquid droplets can move toward higher wettability regions of surface composition gradients, as demonstrated by Chaudhury et al. for a hydrophobic/hydrophilic gradi-

(23) Bain, C. D.; Evall, J.; Whitesides, G. M. *J. Am. Chem. Soc.* **1989**, *111*, 7155−7164.

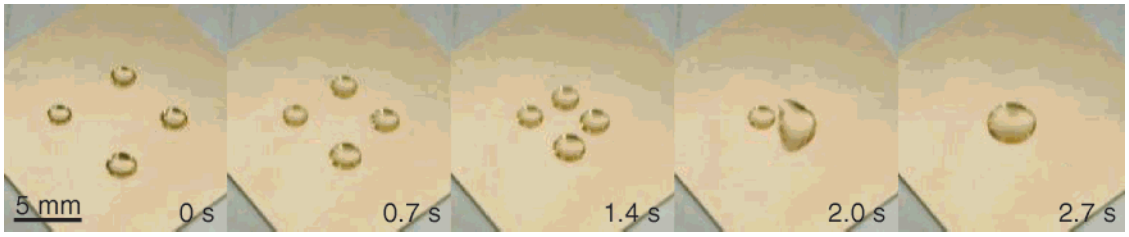

Figure 16. Droplets of heptane moving on radial surface energy gradient. The substrate is vibrated to excite the droplet movement.

ent.[24] The gradients used in our study were all hydrophobic, but changed from oleophobic (PFDDT) to oleophilic (HDT). Droplets of hexane and heptane that were deposited on the fluorinated side should therefore move toward the other end. We performed this experiment with many of our gradients and found consistent movement when the droplets were sufficiently large and the gradient was steep (i.e., obtained from a good stamp). Smaller droplets could be moved on the gradients using vibrational excitation as previously demonstrated by Daniel et al.[25] Figure 16 shows still images from the movement of heptane droplets on a radial gradient, excited by a vibration of the substrate. In contrast to the in-plane movement investigated by Daniel et al., we chose a surface-normal vibration to simplify the observation of the system. It was possible to introduce sufficient energy to overcome the hysteresis at relatively low amplitudes (down to tens of micrometers) when we tuned the vibration to the eigenfrequency of the drop. The supporting material contains a video of a droplet moving on a linear gradient without vibrational excitation.

4. Conclusions

We have shown how to use the mass transfer limitations in the μCP process to print surface composition gradients. Thin stamps that are fully depleted during printing allow the amount adsorbed at any point of the covered surface to be controlled. Such stamps can be prepared in advance with a wide range of gradient shapes and contours to allow a rapid and reproducible gradient fabrication. Although we prepared gradients with a length of about 15 mm, our mass-transfer calculations show that even gradients below 1 mm in length can be printed. The limiting factor is the fabrication of the stamp.

Gradients printed in this work rely on stamps with geometries that enhance surface-normal diffusion paths rather then lateral diffusion. This leads to an almost direct relation between the stamp thickness and the surface composition profile. As microfabrication and conventional high-precision machining today enable the creation of a huge variety of surface geometries, we can print almost arbitrary shapes. Printing does not become more complicated even for very complex shapes, in contrast to most other known methods.

If one does not have the possibility to fabricate the curved molds needed for complex gradients, stamp geometries that include steps and allow a controlled amount of lateral diffusion provide an alternative. The resulting shapes can be predicted relatively easily by using the methods discussed in this paper. On the other hand, thin, entirely flat stamps can transfer a well-defined amount of substance to a defined region uniformly. As they do not contain any thiol after the printing, lateral diffusion that limits the resolution of conventional μCP[26] is minimized.

Many other systems besides the material combination used here (a thiol in a silicone elastomer) could be employed analogously to print other species. For example, hydrogels can be used to fabricate stamps that take up proteins.[27] The combination with the method presented here would allow one to print arbitrarily shaped protein gradients.

5. Experimental Section

Chemicals Used. Hexadecanethiol (Fluka, ≥95%) was used as received. Solutions of HDT in ethanol (absolute ≥99.8%, Fluka, used as received) for inking of stamps were prepared with the highest possible precision and stored at 4 °C for a maximum of one week before use. 1H,1H,2H,2H-Perfluorododecanethiol CF_3-$(CF_2)_9(CH_2)_2SH$ was available from previous studies. It was dissolved in dichloromethane (≥99.8%, Fluka, used as received). Heptane (puriss. p.a. ≥99.5%, Fluka) was used as received.

Sylgard 184 (Dow Corning, Midland, MI) poly(dimethylsiloxane) prepolymer was used to prepare some of the stamps. Other stamps were made from the same mixture with an addition of extra catalyst (platinum-divinyltetramethyldisiloxane complex in xylene, Gelest, PA).

Fabrication of PDMS Stamps. Very thin stamps suitable for the method were fabricated with a precise thickness variation from PDMS via molding.

Ultrathick resist (SU-8 type 10, micro resist technology, Berlin, Germany) was spin-coated onto a silicon wafer to a thickness of 50 μm and patterned using standard photolithography so that rectangular areas of 10 mm by 15 mm were removed. The wafer was cut into individual pieces, mounted on a goniometer, inclined, and polished until all resist was removed on one side but none on the other. The resulting wedge-shaped mold was then fluorinated and filled with the modified PDMS prepolymer mixture. A thin glass slide was pressed onto the mold, and the polymer was left for curing at room temperature. The glass layer improves handling of the finished stamp, which strongly adheres to it.

Use of the modified PDMS instead of the standard commercial product was necessary because a component of SU-8 seems to inhibit the curing process. The diffusion properties of PDMS are likely not to be affected by the addition: full cross-linking is reached both in normal PDMS in the absence of an inhibitor and in the modified PDMS, for the latter even in the presence of an inhibitor.[28]

Additional molds were made by conventional machining. A wedge-shaped mold (50 μm at its thick side) was milled from an aluminum block and a radial mold (100 μm at its center) was turned from an aluminum shaft of 30 mm in diameter. The wedge-shaped mold was polished, teflonated, filled with PDMS, and closed with a glass slide to be left for curing at 60 °C. The radial mold was treated with an adhesion promoter (Dow Corning primer 92−023), filled with PDMS, and cured. The silicone

(24) Chaudhury, M. K.; Whitesides, G. M. *Science* **1992**, *256*, 1539−1541.

(25) Daniel, S.; Chaudhury, M. K. *Langmuir* **2002**, *18*, 3404−3407.

(26) Delamarche, E.; Schmid, H.; Bietsch, A.; Larsen, N. B.; Rothuizen, H.; Michel, B.; Biebuyck, H. *J. Phys. Chem. B* **1998**, *102*, 3324−3334.

(27) Martin, B.; Brandow, S.; Dressick, W.; Schull, T. *Langmuir* **2000**, *16*, 9944−9946.

(28) Kloter, U.; Schmid, H.; Wolf, H.; Michel, B.; Juncker, D. High-resolution patterning and transfer of thin PDMS films: fabrication of hybrid self-sealing 3D microfluidic systems. In *17th IEEE International Conference on Micro Electro Mechanical Systems. Maastricht MEMS 2004 Technical Digest*, *IEEE Catal. No. 04CH37517.*; IEEE: Piscataway, NJ, 2004.

elastomer shrinks during the cross-linking and assumes a concave bow in the stamp surface. This dip was backfilled with PDMS so that the surface could make conformal contact to a substrate.

All stamps were immersed in copious amounts of ethanol to extract short-chained PDMS. They were thoroughly dried in nitrogen prior to use.

Inking of PDMS Stamps. The stamps were imbued with hexadecanethiol so that they contained just the right amount of thiol for our process. Three-millimeter-thick PDMS slabs (ca. 25 × 25 mm in size and 2 g in weight) were extracted in ethanol and then used as "ink pads". Ethanolic HDT solution was dispensed onto one of the stamps, and a second one was placed on top so that the liquid spread at the interface. A dry nitrogen stream removed the ethanol in about 20 min. The ink pads were left in darkness under argon for at least 24 h to allow complete equilibration to an uniform concentration as required in the PDMS stamps. The pads provide a reservoir of virtually constant concentration to the stamps placed on top of the pads. After at least another 12 h, the stamps were ready for printing.

Printing of Gradients. A freshly gold-coated wafer (40 nm gold on 3 nm titanium on a 0.5-mm silicon wafer) was cut into pieces, and particles were removed with a stream of dry nitrogen. The stamp was removed from its ink pad, placed on the substrate, pressed down slightly until contact was established throughout the entire stamped area, left for 3 min, and removed from the gold. Immediately afterward, the sample was treated with a solution of the complementary thiol, washed with ethanol and dried with nitrogen.

Preparation of Reference Samples. Reference monolayers were prepared from HDT solutions (1 mg/mL) in ethanol and PFDDT solutions in dichloromethane (0.4 mg/mL). The same substrates as used in the printing were immersed in the corresponding solution and rinsed with the appropriate solvent after about 3 h.

X-ray Photoelectron Spectroscopy. Spatially resolved analysis of the stamped gradients was done by X-ray photoelectron spectroscopy (XPS) using a VG Scientific Sigma Probe spectrophotometer at a base pressure of about 10^{-7} Pa with a monochromated Al Kα X-ray source ($E = 1486.6$ eV). The X-ray was focused onto an ellipsoidal spot (the long half-axis was 1 mm, the short half-axis was 600 μm in length), and the detector was mounted at an angle of 37° to the sample. The long half-axis of the spot was always at a 45° angle to the gradient direction.

Spectroscopic Ellipsometry. Ellipsometry measurements shown here were made with a Variable Angle Spectroscopic Ellipsometer (VASE) and have been analyzed with the WVASE software (both from J. A. Woollam Co., Inc.). The source used is an arc-xenon lamp with a spot diameter of 1 mm. The measurements were performed using wavelengths from 400 to 1000 nm at 65, 70, and 75°. For our purpose, the incident angle of 70° turned out to be the most sensitive.

After substrate characterization, we prepared and measured pure HDT and PFDDT monolayers. A model of the references was created to find their optical indexes. In a second step, we created a gradient on the substrate and performed a mapping in millimeter steps. The data were then fitted using a Bruggeman effective medium approximation model (consisting of inclusions of one material dispersed in a host matrix of the other), and the composition was determined from the fit.

Profilometry. A Dektak V 200-Si profiler (Veeco, NY) provided stamp profiles. The indentation load on the needle was set to 3 mg. All scans were done in the center of the stamp.

Moving Droplets. Drops of heptane or hexane, typically around 2 mm in diameter, were deposited on the gradient from a capillary. In some cases, notably for the radial gradient shown here, the samples were clamped onto a homemade stage that sat on top of a commercial electromechanical vibrator (Frederiksen, Denmark). This setup allowed us to introduce vibrational movement along the surface normal of the substrate. A frequency generator and an NF-amplifier drove the vibrator with a sine wave at around 100 Hz, manually tuned to the eigenfrequency of the drops.

Acknowledgment. We thank Marilyne Sousa for ellipsometry measurements and Emmanuel Delamarche for useful discussions. A part of this project was funded by the Swiss Commission for Technology and Innovation. The partial support of the Swiss Federal Office for Education and Science (OFES) in the framework of the EC-funded project NaPa (Contract No. NMP4-CT-2003-500120) is gratefully acknowledged. The content of this work is the sole responsibility of the authors. The authors thank Walter Riess and Paul Seidler for their continuous support.

Supporting Information Available: Error estimation for XPS measurements, finite element analysis, and free thiol at the end of stamping as well as a brief movie. This material is available free of charge via the Internet at http://pubs.acs.org.

LA0506527